Postprint of: Głowacki M., Ficek M., Sawczak M., Wcisło A., Bogdanowicz R., Fluorescence of nanodiamond cocktails: pH-induced effects through interactions with comestible liquids, FOOD CHEMISTRY, Vol. 381 (2022), 132206, DOI: 10.1016/j.foodchem.2022.132206

Fluorescence of nanodiamond cocktails: pH-induced effects through interactions with comestible liquids

Maciej J. Głowacki [a], *Mateusz Ficek* [a], *Mirosław Sawczak* [b], *Anna Wcisło* [c], *and Robert Bogdanowicz* [a]*

[a] Gdansk University of Technology, 11/12 G. Narutowicza St., 80-233 Gdansk, Poland
[b] Polish Academy of Sciences, Szewalski Institute of Fluid-Flow Machinery, 14 Fiszera St., 80-231 Gdansk, Poland
[c] Department of Analytical Chemistry, Faculty of Chemistry, University of Gdansk, 63 Wita Stwosza St., 80-952 Gdansk, Poland

*__Corresponding author:__ E-mail: rbogdan@eti.pg.edu.pl. Tel: +48-58-347-15-03. Fax: +48-58-347-18-48 (Robert Bogdanowicz)

Abstract

Fluorescent nanodiamonds with nitrogen-vacancy centers have become important nanoscale probes for sensing and imaging. The surface chemistry of the nanodiamonds influences their emission, interactions, and quantum properties. In this work, we propose to utilize fluorescent nanodiamonds as photostable markers for investigation of comestible liquids. We prepared nanodiamond/comestibles suspensions/cocktails with a wide range of pH levels and studied the samples via fluorescence, wettability, and zeta potential. The composition of the created cocktails revealed a strong impact on the properties of the nanodiamond and its surface chemistry, mainly induced by pH but also tuned by specific quenching compounds. Moreover, the stability of the nanodiamonds in the cocktail media was studied, along with various nature-originated compounds influencing their surface termination, polarity, and charge states. Thanks to the stability and biocompatibility of the nanodiamond, it can be applied in monitoring the condition of foodstuffs, and in the detection of toxins and pathogens in them.

Keywords: nanodiamonds; nitrogen-vacancy centers; liquid comestibles; fluorescence, markers

1. Introduction

Nanodiamonds (NDs) are a class of diamond structures with sizes not exceeding 1 μm. More than 10 methods for the production of the nanodiamonds exist with 3 of the techniques performed commercially: a detonation method, high-temperature, high-pressure (HPHT) synthesis followed by milling, and laser ablation. The HPHT procedure is generally preferred for the production of diamonds meant to be used as hosts for the color centers. The centers of a special interest to scientists are nitrogen-vacancy (NV) centers, exhibiting intensive, red fluorescence emission, which is very stable at room temperature and undergoes neither bleaching nor blinking. The zero-phonon lines

(ZPLs) of the neutral (NV^0) and negatively charged nitrogen-vacancy (NV^-) centers appear at 575 nm and 637 nm, respectively (Crane et al., 2019; Panwar et al., 2019).

Interactions of NDs with products suitable for consumption are a research topic that is being turned to increasingly commonly. The nanodiamonds have found application in several techniques used to detect substances from inside comestible products. One such technique is the electrochemical detection, where NDs, along with other forms of carbon, are used to enhance the sensing substrates. Babadi *et al.* (Babadi et al., 2019) developed a composite electrode made of copper, carbon nanotubes and nanodiamonds. The electrode was modified with L-amino acid oxidase and used for detection of amino acids in the *Parkia speciosa* juice. Carvalho *et al.* (Carvalho et al., 2021) coated screen-printed carbon electrode with NDs, and used it in electrochemical immunosensor to track peanut allergen Ara h 1 in samples extracted from an energy bar, cookies and granola. Jiang *et al.* (Jiang et al., 2018) used several different forms of carbon (graphene or amorphous carbon or boron-doped nanodiamond) drop-cast on glassy carbon electrodes for electrochemical sensing of phenolics. The electrodes utilizing the amorphous carbon were used to detect hydroquinone and catechol in green tea samples. Shabnam *et al.* (Shabnam et al., 2017) deposited a composite of copper nanoparticles and nitrogen-doped graphene on a glassy carbon electrode for electrochemical detection of glucose. The detection has been performed in various food products, including tea, concentrated orange juice, sweetened beverages, and energy drinks. Recently, Kumar *et al.* (V. Kumar et al., 2020) manifested direct-current voltage (IV)-based sensor for facile detection of urea in milk samples, utilizing an urease-immobilized graphitized NDs.

Another method for analysis of food products where the nanodiamonds have found wide application is chromatography. NDs are often used as sorbents to enhance the solid-phase extraction of substances from comestible samples. Ozdemir et al. (Ozdemir et al., 2017) reported that *Bacillus altitudinis*-immobilized nanodiamonds could be applied as biofunctional sorbent for preconcentrating of cobalt, chromium or lead cations in food samples toward optimum analytics of their concentrations by ICP-OES. The food products under examination were black tea, onion, cheese, and rice samples. Ulusoy *et al*. (Ulusoy et al., 2019) modified a nanocomposite of multi-walled carbon nanotubes and NDs with Fe_3O_4 nanoparticles. The resulting nanoparticles were used in magnetic solid-phase extraction to detect vitamin B12 in food samples (milk powder, orange and peach juice, salami, and certified reference materials) via high-performance liquid chromatography–photodiode array method. Cui *et al.* (Cui et al., 2019) applied functionalized nanodiamonds as one of the co-monomers in the preparation of a solid-phase extraction column used to enrich and purify ß-sitosterol in four kinds of comestible oils. A small addition of the nanodiamonds ensured uniform porosity and improved the thermal stability of the column. The impact of pH on the efficiency of the biosorption was investigated, and it was reported that the highest recovery rates may be obtained at mildly acidic pH values (5–6).

NDs have also been applied directly inside the food products. Grichko *et al.* (Grichko et al., 2006) demonstrated the potential use of detonation nanodiamonds as carriers of substances promoting or inhibiting the growth of bananas. Delayed ripening was successfully achieved by introducing detonation nanodiamonds coated with diphenylcyclopropenone into the bananas. Some experiments have used food products as precursors in the preparation of carbon nanoparticles. Cong *et al.* (Cong et al., 2019) successfully separated fluorescent, mostly carbon-based nanoparticles from a popular type of pizza. The authors attributed the origin of the nanoparticles to physicochemical reactions occurring during the thermal processing of the food. On illumination with UV light, a suspension of the nanoparticles emitted pH-dependent, blue fluorescence, which shifted toward longer wavelengths as the excitation wavelength was increasing.

Carbonaceous materials are being increasingly added to food packaging as bacteriobic materials. Mitura *et al.* (Mitura et al., 2017) presented that food packaging films modified with carbon nanomaterials can affect the viability of bacteria. Mikamoto *et al*. (Mikamoto et al., 2020) showed improvement in durability and sliding properties of food packaging equipment by combined treatment of diamond-like carbon coating and fine particle bombarding. Arcot *et al.* (Arcot et al., 2021) manifested that nanodiamond-coated high-density polyethylene (HDPE) surfaces show superhydrophobic behavior and reduce the cross-contamination of spinach leaves by *Salmonella typhimurium* and *Listeria innocua* attributed to the water-repellent nature of NDs. The study of the influence of the nanodiamonds on food products is very important due to the possibility of the release of the nanodiamonds from the packaging to the product.

Moreover, food safety monitoring issues have recently attracted big interest, especially the possibility of replacing the conventional high-performance laboratory techniques with point-of-care technology (Choi et al., 2019). The most commonly used detection methods are based on colorimetric and fluorescence measurements. Compared to colorimetric-based test methods, fluorescence measurements enable a significant increase in sensitivity. Different fluorescence techniques based on functionalized polymeric nanoparticles, quantum dots and graphene-oxide-based structures have been reported in application for food contaminants detection (B. Li et al., 2017). The advantages of the nanodiamonds in food testing are their biocompatibility and durability, which allow for long-term use. Moreover, since the color centers can be created inside the nanodiamonds, these particles do not need any additional fluorophores for optical detection.

An issue of the influence of pH on the physical properties of the nanodiamonds, and the nitrogen-vacancy centers in particular, was brought to researchers' attention recently, and it has already given rise to many novel experiments expanding the potential of these structures. Reineck *et al.* (Reineck et al., 2018) analyzed the fluorescence of aqueous suspensions of disaggregated, oxidized detonation nanodiamonds in a range of pH between 3.7 and 12.7. The authors found the intensity of the photoluminescence reaching maximum values in highly alkaline conditions, and decreasing significantly toward lower pH levels, which is similar to the pH dependence of the fluorescence

emitted by aromatic hydrocarbons. The spectra presented by Reineck *et al.* (Reineck et al., 2018) do not contain zero-phonon lines of the nitrogen-vacancy centers. Fujisaku *et al.* (Fujisaku et al., 2019) focused on the impact of pH on the value and decay of a longitudinal relaxation time (T_1) of NV^- electron spin. The authors analyzed carboxylated nanodiamonds under a pH of range of 3–11, and found the dependence of T_1 on the surrounding pH between values of pH=3 and pH=7, but not between pH=7 and pH=11. Satisfactory reversibility of T_1 was also established when the ambient pH was alternated between pH=3 and pH=9 (Fujisaku et al., 2019).

Extensive research on application of the nanodiamonds as bioimaging agents and markers of local temperature or magnetic field monitoring requires an understanding of their functioning in various environments with different pH values. Due to their biocompatibility, NDs can be used to monitor the condition of food, the content of toxins, and to detect pathogens in them (Białobrzeska et al., 2021). Next, fluorescent NDs could be considered as a functional optical marker or sensing agent in food products and packaging (see Table S1 in the Supplementary Information). The readout of NDs' fluorescence allows for targeted determination of food quality or detection of contamination or hazardous compounds, enabling qualitative and quantitative production of healthier, safer, and high-quality functional food (Medeiros et al., 2010). NDs could also be used as a synergistic agent in smart food packaging, enabling fluorescent monitoring of the quality of the stored food and increasing shelf-life of food products once modified by active groups working as preserving agents (Arcot et al., 2021). Therefore, we examined the fluorescent parameters and NV charge manipulation of NDs in selected comestible liquids across a wide pH range for the first time. The stability of nanodiamond particles in real comestible liquids was also particularly studied. There are studies available in the literature proving the usefulness of wettability parameters in the assessment of food products - i.e. the characteristics of multi-component solid foods, providing information on the migration of fats in chocolate, and also allowing for the evaluation of capillary flow as a migration mechanism (Reinke et al., 2015) (see details in S1.2. section in the Supplementary Information).

In the present study, commercially available NDs containing NV color centers were dispersed in a series of comestible liquids varying in pH and composition. Comestible liquids are complex media consisting of various nature-originated compounds influencing NDs' surface termination, as well as their polarity and charge states. In order to verify whether NDs may be easily, unambiguously detected optically from within the comestible liquids, the measurements of fluorescence were carried out. The obtained spectra were analyzed in search of characteristic local maxima (peaks) exhibited by NV centers, i.e., ZPLs and phonon sidebands. Moreover, to evaluate sensing possibilities of NDs via fluorescence spectroscopy, a ratio of photon count rate at ZPL of NV^- centers to the photon count rate at ZPL of NV^0 centers was calculated where possible, and compared to data obtained for a reference series of suspensions of NDs in deionized water, with pH tuned either with HCl, or NaOH. This has been to verify whether pH is a crucial property of the media to potentially influence the fluorescence of NV centers, or whether the centers are more affected by the composition of their surrounding comestible environment. To assess the stability of the systems, zeta potential of the suspensions of NDs in the comestible liquids has been examined.

Furthermore, measurements of contact angle between droplets of the suspensions and a surface made of polytetrafluoroethylene (PTFE) have been carried out.

2. Materials and methods

2.1. Nanodiamond suspensions

The suspensions were prepared by dispersing commercially available, fluorescent carboxylated diamond particles (ND-COOH, Adámas Nanotechnologies, approximately 700 nm average particle size, 3.5 ppm concentration of NV^- centers) in a variety of liquids. As a preliminary step, the diamond powder itself was characterized using Raman spectroscopy and scanning electron microscopy (SEM). For this purpose, it was suspended in deionized water, and then drop-cast onto a silicon substrate and dried to form a thin layer.

The following 8 comestible liquids were selected to prepare the nanodiamond suspensions: 10% spirit vinegar, 100% lemon juice, 100% apple juice, 100% beetroot juice, 100% coconut water, black tea, green tea, and alkaline mineral water. Information regarding the producers of the comestible liquids is presented in Table 1. The liquids were always bought on the day of the experiment and unpacked directly before the synthesis procedure in order to maintain the maximum freshness of the products. Except for during the synthesis and the measurements, the samples were stored in a laboratory refrigerator.

The fluorescent powder was separately added to each of the liquids to obtain a 0.1% mass concentration of the diamond. The samples were then treated in an ultrasonic bath for 30 minutes to ensure homogeneous dispersion of the particles. The pH of the samples was measured directly after the synthesis. The names of the suspensions and their corresponding dispersion media are presented in Table 1. The samples were examined in terms of fluorescence and zeta potential. Additionally, the measurements of the contact angle between droplets of the suspensions and a surface made of polytetrafluoroethylene (PTFE) were carried out.

Table 1. Details on the origins, and initial pH values of the comestible liquids, as well as pH values of the resulting nanodiamond suspensions

Comestible liquid	Producer	Symbol of the comestible liquid	Initial pH of the comestible liquid	Symbol of the suspension based on the comestible liquid	Resulting pH of the suspension
10% spirit vinegar (V)	OCTIM Sp. z o.o., Poland	V	2.33	V-NV-ND	2.33
100% lemon juice (L)	Polenghi LAS s.r.l., Italy	L	2.52	L-NV-ND	2.48
100% apple juice (A)	Tymbark - MWS Sp. z o.o. Sp.k., Poland	A	3.50	A-NV-ND	3.48

100% beetroot juice (B)	Excellence S.A., Poland	B	4.43	B-NV-ND	4.45
100% coconut water (C)	N.B. Value Link Co. Ltd., Thailand	C	5.25	C-NV-ND	5.23
Green tea (GT)	Unilever Polska Sp. z o.o., Poland	GT	7.18	GT-NV-ND	7.42
Black tea (BT)	Unilever Polska Sp. z o.o., Poland	BT	7.32	BT-NV-ND	7.59
Alkaline water (AW)	Zbyszko Company S.A., Poland	AW	8.42	AW-NV-ND	8.99

The reference series of the suspensions were based on simple inorganic liquids. By mixing the deionized water either with 0.1M hydrochloric acid (HCl), or 0.1M sodium hydroxide (NaOH), 11 solvents having consecutive integer values of pH in the range of 2.00–12.00 were prepared. Separately an aqueous nanodiamond suspension with a 0.2% concentration of the particles was made using an ultrasonic bath. An equal portion of the suspension was added to each of the prepared solvents in a 1:1 volume ratio, thus creating a series of samples with identical content of the diamond and pH in the range of 2.39–11.67. The fluorescence of the suspensions was thoroughly measured and compared with the photoluminescence emitted by the suspensions based on the comestible liquids.

2.2. Control of pH

The pH of the suspensions was examined using a Mettler Toledo pH meter equipped with an InLab Expert Pro-ISM electrode. The electrode was carefully rinsed with deionized water before the measurement of any next sample.

2.3. Raman spectroscopy

Raman spectra were recorded utilizing a micro-Raman spectrometer (Invia, Renishaw) with 514 nm argon-ion laser excitation. The samples were analyzed in the form of a suspension drop-cast on a silicon substrate. Additionally, the drop-cast suspension was dried and the nanomaterial was analyzed in the form of a thin film deposited on a silicon surface.

2.4. Fluorescence setup

Laser-induced fluorescence spectra were recorded using a laboratory built system consisting of a 532 nm Nd:YAG SHG laser (Millenia, Spectra-Physics) excitation source operating at a power level of 0.2 W. The fluorescence spectra were recorded employing a 0.3 m monochromator (SR303i, Andor) equipped with a 600 grove/mm grating and ICCD detector (DH740, Andor). Liquid samples (suspensions) were analyzed in quartz cuvettes excited from the front side with a laser beam at an angle of 45 degrees. The fluorescence signal was collected perpendicular to the cuvette wall illuminated with the laser using a quartz lens end focused on the entrance of an optical fiber. In the detection path, a band-pass filter (OG570, Schott) was used to block the laser radiation.

2.5. Zeta potential

The zeta potential of the samples was measured at 25°C using a Zetasizer Ultra (Malvern Panalytical Ltd.). Due to the limited transmittance of the beam caused by the high opacity and intensive scattering of the suspensions, a cell with palladium electrodes was applied for highly concentrated samples.

2.6. SEM imaging

Microscopic measurements of the starting diamond powder deposited onto a silicon substrate were carried out using a HITACHI S-3400N scanning electron microscope. The particles were visualized using the detection of secondary electrons. The accelerating voltage of the beam was equal to 25.0 kV.

2.7. Contact angle measurements

The contact angle measurement technique is based on measuring the contact angles of drops of tested liquids and the surface of known materials. In this case, we used PTFE because this material's surface energy is 18 mN/m and is fully dispersive. A drop of 2 μL of probe liquid was deposited using a syringe and the image of the drop was captured by a CCD camera connected to a graphics card. Measurements were repeated 30 times. After digital image analysis, the average contact angle was deduced by the Young-Laplace method from the angles measured at both sides of the drop in equilibrium. The total surface tension for these liquids was obtained with the pendant drop method, which is equivalent to the sessile bubble method. A small droplet of a tested liquid is suspended from a steel needle (capillary tube). The surface tension is derived from the fitted contour of the drop shape. The dispersive and polar parts of the surface tension of the liquids were calculated from contact angle measurements on the PTFE and the surface tension measurements with the use of Eq.(1).

$$\gamma_L^D = \left(\frac{\gamma_L^2}{72}\right)(cos\theta_{PTFE} + 1)^2 \quad (1)$$

Where $cos\theta_{PTFE}$ is the contact angle of the tested liquid measured on the PTFE; γ_L^D - is the dispersive part of surface tension, and γ_L^2 is its surface tension. The polar part is calculated by the difference between the surface tension and dispersive part.

3. Results and discussion

3.1. Morphology and structure of NV-rich nanodiamonds

Fluorescent carboxylated nanodiamonds (ND-COOH) were utilized to study their behavior in selected comestible liquids shown in Figure 1 and listed in Table 1. ND-COOH particles showed standard structure as revealed by Raman spectra in aqueous suspension or dried on a Si wafer (see Fig. S1 in the Supplementary Information). Both specimens exhibited sp^3 diamond peak accompanied with a G band, although the dried samples manifested much lower sp^3 peak intensity thanks to the decrease of their effective volume.

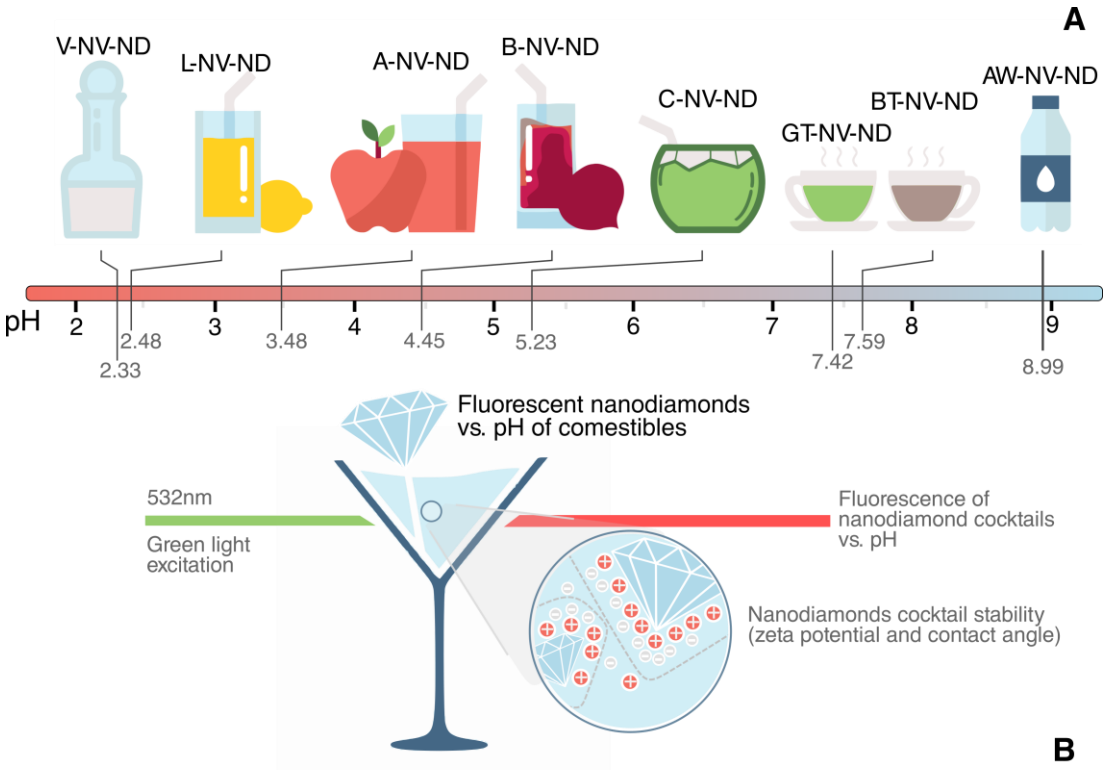

Figure 1. Overview of studied NV-ND suspensions/cocktails: A) Overview of studied comestible liquids along with pictograms of the NV-ND suspensions with referring pH values: 10% spirit vinegar; 100% lemon juice; 100% apple juice; 100% beetroot juice; 100% coconut water; black tea; green tea; alkaline mineral water; B) Principles of conducted investigations of the nanodiamond cocktails, where the fluorescence and stability of the suspensions were tailored by pH of specific surrounding comestible.

The SEM micro-images present the morphologies of the dried NV-ND suspensions based on ND-COOH and the various comestible liquids, mimicking a wide range of pH. The bare NV-ND particles were shown for reference (Fig. 2A). The representative dried suspensions of NV-ND, widely spread from highly acidic spirit vinegar (Fig. 2B) through green tea (Fig. 2C) up to alkaline water (Fig. 2D), revealed an increased effect of agglutination. Since the diamond grains originated from the HPHT method, crushed to form a fine powder of NDs, their shapes are far from spherical. The longitudinal dimensions of the nanodiamonds noticeably agglutinated in Figs 2C and 2D are similarly in the range of 3–5 μm, with the majority of the particles having the size of 700–800 nm. The ND agglutinates exhibit a kind of core-shell softened morphology probably induced by spirit vinegar and green tea residuals. The dynamic light scattering (DLS) measurement indicates that a higher pH of the comestible liquid induces an increase of the ND-COOH sizes, as reported in the artificial buffers with increasing of pH (Lei et al., 2016).

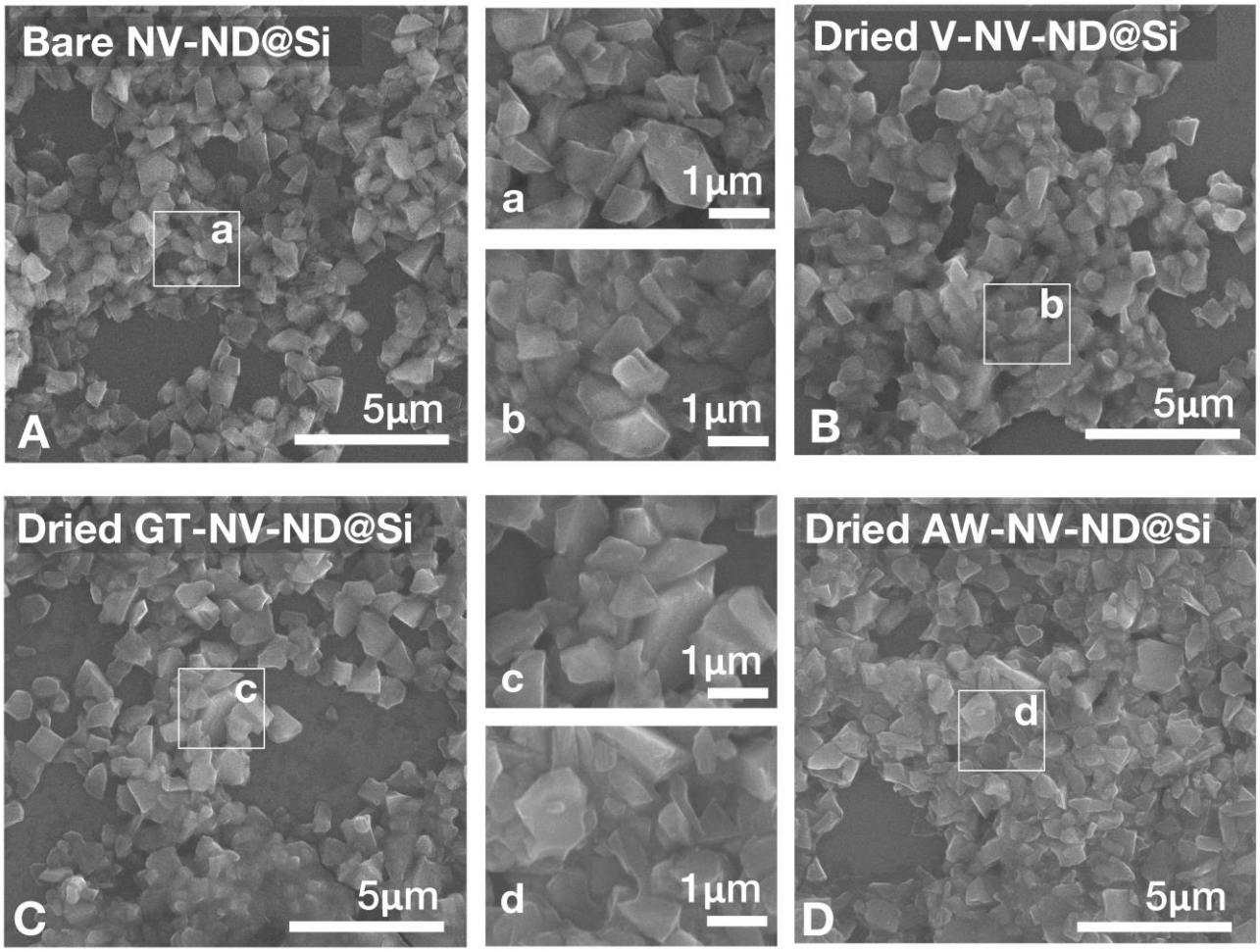

Figure 2. SEM morphologies of dried NV-ND suspensions based on: A) deionized water (reference); B) 10% spirit vinegar; C) green tea; D) alkaline mineral water.

Conversely, the reference, bare NV-ND forms groups with exposed sharp crystal edges while dried on Si. Figure 2D reveals that alkaline water (pH ~9) induces the most intensive ND aggregation effect, where almost all ND particles are agglutinated. This effect was attributed to the variations of electrostatic forces between the NDs as manifested priorly in various electrolytes (Fujisaku et al., 2019). It was previously reported by Fujisaku *et al.* (Fujisaku et al., 2019) that the size of aggregates of fluorescent nanodiamonds increases for pH ~9, exhibiting larger hydrophobicity caused by surficial groups protonation and consequently influencing NV center emission.

The -COOH surface groups on the ND particles are strongly pH-dependent, tending to undergo ionization in specific media, while shape differences or differences in sizes of ND agglutinates (see Fig. 2) could be indirectly ascribed to the pKa of the selected comestible liquids (D. G. Lim et al., 2016, 2020). The ionization process of -COOH groups achieves negative charges in alkaline pH, inducing repulsion of the nanodiamond particles, and accordingly a reduction of the sizes of the ND agglutinates. Reineck *et al.*(Reineck et al., 2018) found that a higher pH promotes a ND minor aggregation effect at pH = (8–10) and a rapid effect above pH ~11. Such a process was

ascribed to adsorption of shielding Na^+ ions reducing electrostatic repulsion among the NDs observed indirectly by a zeta potential decrease (Reineck et al., 2018).

3.2. Studies on the pH-dependency of the fluorescence and zeta potential of NV-rich nanodiamonds suspended in comestible liquids

Fig. 3A displays the fluorescence spectra of the nanodiamonds suspended in the comestible liquids with a pH in the range of 2.33–8.99. The signals emitted by the NV-ND suspensions have been corrected with spectra recorded for the pure comestibles (Fig. 3B), therefore Fig. 3A depicts the photoluminescence spectra of the nanodiamonds themselves. The signal emitted by the particles dispersed in 10% vinegar completely overlaps with the fluorescence spectrum of the nanodiamonds suspended in alkaline water. In 7 out of 8 cases, the spectra contained visible local maxima at 637 nm, which are ZPLs of NV^- centers, as well as significantly weaker maxima at 575 nm (ZPLs of NV^0 centers). The beetroot juice appears to be completely suppressing the photoluminescence exhibited by the color centers. There seems to be no monotonic trend in the intensity changes of the fluorescence spectra recorded for ND suspensions prepared at various pH induced by specific comestibles. Interestingly, the strongest signal was collected from the particles suspended in the lemon juice and the apple juice – two highly acidic liquids.

This stands in noteworthy contradiction to the reference series and the previously reported research focused on the optical performance of nanodiamonds in diverse pH (Reineck et al., 2018). However, it is important to notice that in the present experiment, the dispersion media are very complex, mostly organic liquids that may interfere with the color centers, either tuning or quenching their photoluminescence. It should be noted that negatively charged NDs (Fig. 3D) were found to be more resistant to pH-induced aggregation in comparison to positive nanodiamond particles with a zeta potential higher than 30 mV (Bradac et al., 2018).

There is also a clear influence of the comestible composition on the fluorescence pattern and intensity. For future analysis, the spectra presented in Fig. 3A were corrected with the corresponding spectra recorded for the reference comestibles, and the ratio of photon counts at the ZPL of NV^- to the ZPL of NV^0 was analyzed (Fig. 3C). The results were compared to data obtained for the set of reference samples prepared with nanodiamond suspension and deionized water solution with the pH tuned either with HCl, or NaOH. In the case of the reference samples, the monotonic increase of the level of the NV^-/NV^0 with an increase of pH is observed and is consistent with the results obtained for the detonation nanodiamond fluorescence vs pH reported by other authors (Reineck et al., 2018). Next, the NV color centers could be influenced by a pH range of 3–7 but minor changes in emission were recorded in the range pH 7–11 as reported by Fujisaku *et al.* (Fujisaku et al., 2019).

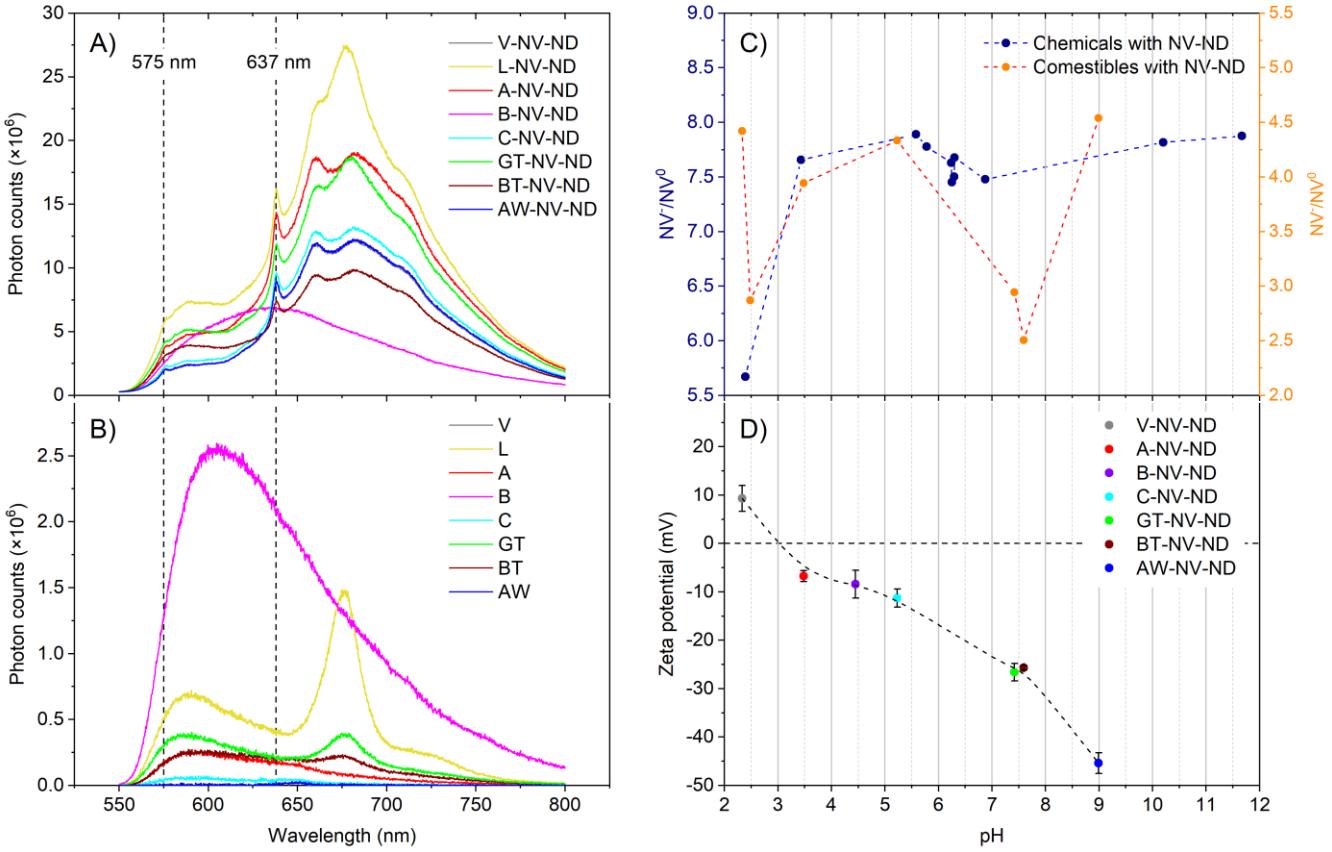

Figure 3. A) Fluorescence spectra of the nanodiamond suspensions based on the comestible liquids; B) Fluorescence spectra of the comestibles before the addition of the diamond powder; C) ratio of the photon count rate at 637 nm (ZPL of NV^- centers) to the photon count rate at 575 nm (ZPL of NV^0 centers) versus pH for the suspensions based on the comestible liquids and inorganic chemicals; D) zeta potential of the suspensions based on the comestibles versus their pH.

The drop of fluorescence observed for pH near 6.3 is induced by the rapid deprotonation process of the nanodiamond surface (Fujisaku et al., 2019). While the NV^0 fluorescence is independent of external factors, the NV^- centers are sensitive to a magnetic field, pH, and their potential application as sensors is being intensively studied (Bhaumik et al., 2019; Rondin et al., 2010). For the sensing application, the NV^- centers located near the diamond surface are being considered and in the case of pH variation, the changes in the fluorescence intensity can be explained with protonation and deprotonation processes of surface groups. The decrease of pH causes protonation processes that also lead to an increase in the zeta potential (Reineck et al., 2018). In the case of samples containing a nanodiamond suspension combined with complex organic comestibles, the interference of pH and the influence of different comestible compounds caused processes that influence the fluorescence signal, however the dependence of the intensity of the fluorescence vs pH for selected samples is comparable with that observed for the set of calibration samples – Figure 3C. For selected comestibles (vinegar, black tea, green tea), the compounds present in its composition interfere with the fluorescence of the NV centers, resulting in fluorescence quenching

(black and green tea) or overlapping the signal from the nanodiamonds. Moreover, the pH influence on the fluorescence could also be reorganized by excited-state proton transfer processes (Reineck et al., 2018; Zelent et al., 2006). The strong enhancement of the emission of carbon dots, being a kind of ND analog, was observed when lemon juice was tested (Dutta Choudhury et al., 2017). Furthermore, the analytical analyses of lemon juice exhibited a variety of compounds such as acetic, lactic, malic, ascorbic, and citric acids that drive a boost of luminescence (Gargouri et al., 2017). The increase of suspension electrical conductivity and wettability could be ascribed to the observed intensity enhancement, where more electrons are highly excited forming radiative electron-hole pairs and facilitating improved fluorescence. Sacksteder *et al.* (Sacksteder et al., 1990) reported that citric acid could even double the emission of quinine solution observed as a flattened Stern-Volmer plot and driven by the kinetics of excited states.

The decrease of the fluorescence of the black tea solution could also be attributed to the presence of catechin (Du, Ma, Gu, Li, Zhu, et al., 2020) or theaflavin (Wu et al., 2020) in the supernatant, which are also known as static quenchers. Moreover, the caffeine in the black tea could also interact with the fluorescent nanodiamonds, capturing free protons and creating π-stacking (Du, Ma, Gu, Li, & Chen, 2020), which would also reduce fluorescence. Next, Miao *et al.* (Miao et al., 2015) revealed that the green tea extract could also form complexes inducing the static quenching mechanism due to epicatechin gallate (found in the extract) involving probable binding with the nanodiamonds and Van der Waals forces. Additionally, the complex composition of coconut water, containing among others, vitamins, sugars, amino acids, proteins, and lipids, could suppress effective non-covalent energy transfer and, thus reduce ND fluorescence.

The strong influence of beetroot juice could be mainly attributed to the betanin pigment and its derivatives present in the natural extract (Das et al., 2020) exhibiting fluorescence quenching for even micro-molar concentrations of betalains. Gliszczyńska-Świgło *et al.* (Gliszczyńska-Świgło et al., 2006) found pH-dependent intensive free radical scavenging activity of betanin, which could be an additional factor causing deprotonation of -COOH groups at the surfaces of the fluorescent NDs.

Metal ions such as Sn(II) and Zn(II) (Y. Li et al., 2020) that exist in juices and alkaline water could also reveal fluorescence-quenching behavior when weakly bonded or adsorbed to the NDs' surface thanks to the spin-orbit coupling energy or electron transfer. Lastly, ascorbic acid (Vitamin C) is widely present in fresh fruit juices and is responsible for a photo-induced electron transfer mechanism that also causes fluorescence quenching.

The reduction of the average size of the NDs would also cause photoluminescence of NVs thanks to the annihilation of vacancies. Tsapyuk *et al.* (Tsapyuk et al., 2020) reported that sonication treatment triggers C-O bonds, thus defects or color centers linked to oxygen-containing surface groups such as -COOH would be significantly altered. Obviously, the deprotonation considerably enhances the charge of the oxygen atoms in the -COOH groups, increasing the negative surface charge of the NDs and thus decreasing the trend of particle aggregation. Deprotonated ND-COOH surfaces exhibit a large negative charge creating a dense hydration shell around particles

by surrounding H_2O, which quench fluorescence. Nevertheless, Fujiwara *et. al.* (Fujiwara et al., 2019) revealed a minor influence of pH on the final response of NV-based quantum sensors, where just a slight weakening or response could be attributed to water adsorption initiating the photoionization of charge states in nitrogen vacancies.

Fig. 3D depicts the zeta potential of the NDs suspended in the comestible liquids versus the pH in the range of 2.33–8.99. The signal transmitted through the sample based on the lemon juice was below the noise level, even though a special cell for highly concentrated liquids was used. Therefore, this one suspension is not included in the graph. The value of the zeta potential of the nanodiamonds is positive for highly acid media (pH < 3.00) and negative for higher pH, which is typical behavior. The isoelectric point occurs at pH = 3.00. In the case of the samples based on vinegar, apple juice, beetroot juice, and coconut water, the absolute value of their zeta potentials is below 25 mV, and therefore these suspensions cannot be considered stable, as the diamond particles will eventually undergo sedimentation. The sample based on alkaline water is characterized by the highest absolute value of the zeta potential, equal to 45.4 mV, and regarded as an indicator of good stability (A. Kumar & Dixit, 2017). Evidently, the changes in pH values induce variation in the hydrodynamic diameter of ND-COOH agglutinates, which could be observed by DLS or in a decrease of the zeta potential (D. G. Lim et al., 2016, 2017). Lim *et al.* (D. G. Lim et al., 2020) reported a negative zeta potential of -27.0 ± 0.4 mV for a pH of 8 for ND-COOH being comparable with the data presented here in Fig. 3D. Thereafter, the variation of the zeta potential versus pH reported here, measured for samples containing diamond suspension and comestibles increases with the reduction of the pH, which is in agreement with previous results presented by Reineck *et al.* (Reineck et al., 2018).

3.3. Studies on the dependency of the contact angle of NV-rich nanodiamond suspended in comestible liquids

Various studies were conducted to determine the impact of the presence of the nanodiamonds on the parameters of wettability and surface tension of liquids, taking into account the pH of the tested systems. Such an approach allowed us to gain an understanding of the solvent/nanodiamond interactions driving variations in fluorescence. Figure 4 displays the contact angle and surface tension values of the tested liquids together with the symbols used. The surface tension of the comestible liquids was mostly lower (~54–58 mN/m) than clean water (75 mN/m). Only in the case of apple juice and alkaline water was it slightly higher (~79 mN/m). The admixture of nanodiamond suspensions into these samples generally reduces surface tension. Nevertheless, these changes are not significant enough to indicate the function of nanoparticles as a surfactant. This behavior is closely related to the Brownian motion of nanoparticles within a comestible liquid. This phenomenon causes the diffusion of the nanodiamond particles within the droplet, thereby changing the structure of the liquid-gas interface, which results in a decrease in surface tension.

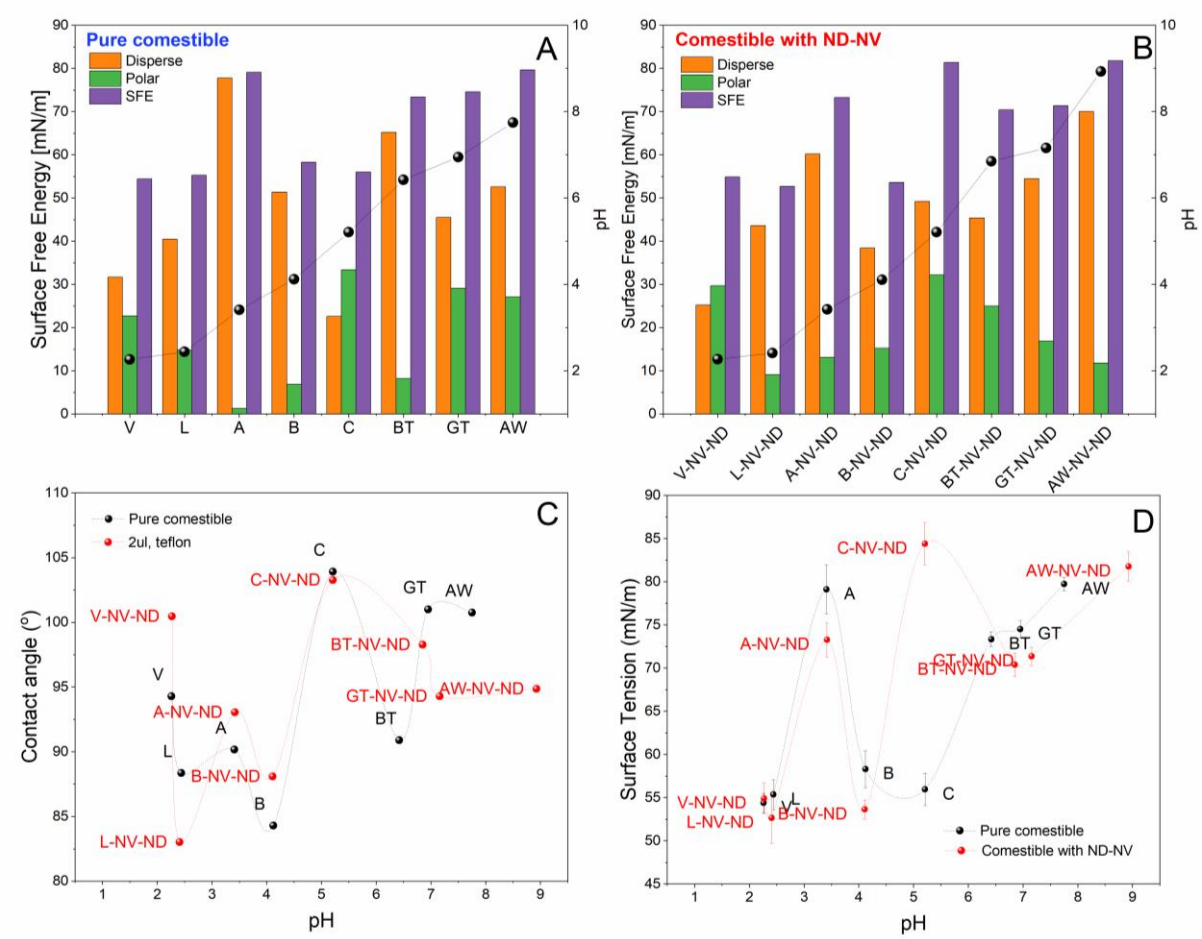

Figure 4. Diagrams of surface energies with uncertainties for: A) the investigated pure comestibles; B) comestibles containing nanodiamonds; C) dependence of contact angle and D) surface tension of investigated liquids on pH.

In addition, the contact angle measurements of pristine and NV-enriched comestible liquids were examined at a standard reference PTFE surface. The achieved results were again compared to ultrapure water. Pristine beetroot juice exhibits the lowest contact angle (84.29°) among the tested comestibles while coconut water (103.91°) possesses the highest. In general, it was noticed that comestibles with an acid nature have lower contact angles at PTFE than those of an alkaline nature. In addition, nearly all of them have improved wettability than ultrapure water. The admixture of nanodiamond suspension increases the contact angle for all of the samples. However, in the case of samples with alkaline pH, we observed the reverse trend of changes. ND suspensions show a lower contact angle than the corresponding sample without nanodiamonds. Such changes in wetting in the presence of NDs seem to be reasonable when looking into the mechanism of the wetting process.

Drop formation on the surface of a solid material depends on many factors. It is at the interface of individual phases – liquid, solid, and gas – that interactions shape the droplet shape. Hence, both the surface tension of the liquid that changes after the addition of NDs, as well as their settling on the surface of the material, ultimately affect the value

of the contact angle. Previous studies of nanoparticle suspensions have shown that as a result of their adsorption on the surface of the tested material, and thus its modification, the contact line of these phases changes, which results in a change in the contact angle (S. Lim et al., 2015; Radiom et al., 2009; Sefiane et al., 2008; Vafaei et al., 2006; Zhong et al., 2015). Moreover, the observed higher hydrophilicity of ND is driven by changes in the total surface energy, which was ascribed previously to the rise of the Lewis acid-base surface tension component (Zhuang et al., 2010).

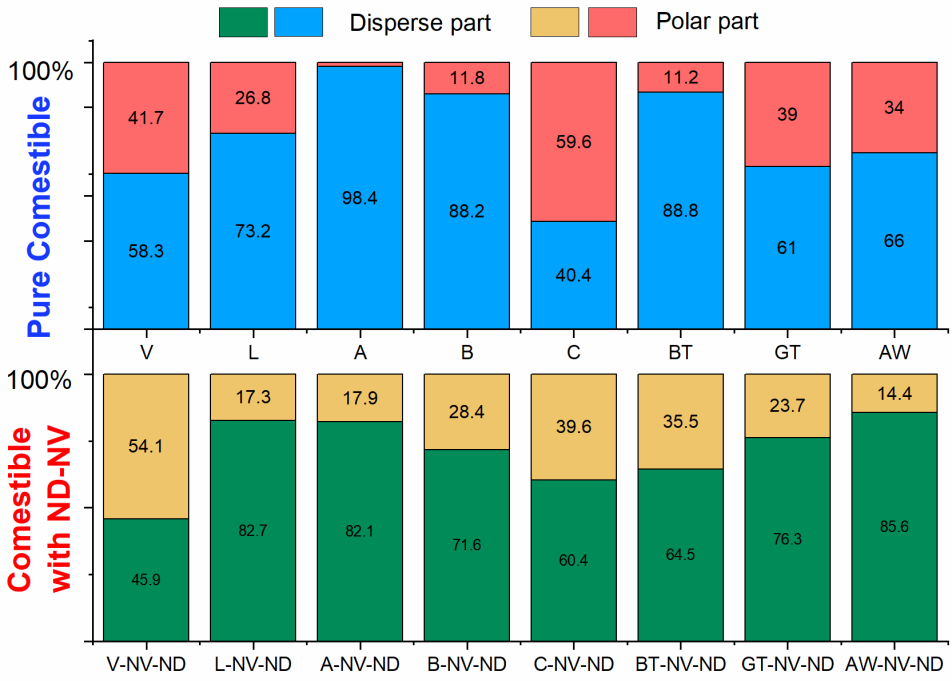

Figure 5. Diagrams of the percentage of the dispersive and polar parts of surface tension (SFT) with uncertainties for investigated comestibles with and without the nanodiamonds.

Moreover, the contact angle measurements on PTFE were performed and the parameters of the free surface energy of the investigated liquids were determined (see Fig. 4). Surface energy is the effect of intermolecular interactions at interfaces, which allows their characterization. It can be divided into two components: disperse (γ^d), attributed to van der Waals and other non-specific interactions, and polar (γ^p), resulting from dipole-dipole, dipole-induced dipole interactions, hydrogen bonds, and other specific interactions at the interface. The total surface energy is expressed by Eq.(2).

$$\gamma^s = \gamma^d + \gamma^p \quad (2)$$

The tested comestible liquids are characterized by energy values in the range of 54–79 mN/m (Fig. 4A). Basically, it can be assumed that this value increases with increasing pH, however, the exception is apple juice, which has the highest value of this energy (79.1 mN/m). Moreover, these liquids have a predominant proportion of the dispersive fraction (40–98%), however, the polar fraction is usually lower by a maximum of half. The apple juice is again

interesting, where practically the entire value of the surface free energy is dispersive (98.4%). Also in the case of beetroot juice and black tea, the dispersion part is significantly dominant (88% both) (Fig. 5). The only exception is coconut water, where the polar part is predominant (59.6%). Introduction of the nanodiamonds mostly increases the proportion of the polar part (Fig. 5). The value of the total energy does not change significantly and is still in the range of 54–81 mN/m. In the case of coconut water, the proportions were completely reversed. The presence of nanoparticles caused the share of the dispersive part to became dominant.

Ostrovskaya et al. (Ostrovskaya, 2002) showed a surface energy of 50 mN/m for similar thin diamond films. Larger values were achieved for microcrystalline diamond films, where higher surface roughness is responsible for an increase of surface energy (~66 mN/m at H-terminated and ~75 mN/m at O-terminated) (Ma et al., 2020). The results obtained here are just slightly larger or analogous to those reported in the literature. Other works reported values for hydrogenated/oxidized thin continuous films. The studied NV-ND aggregates definitely reveal a larger surficial concentration of oxygen-rich groups, which increases the surface energy.

It is worth noting that higher pH along with increased ionic strength induces higher forces leading to adsorption of nanoparticles at solvent interfaces (Ferdous et al., 2012). The simulations of the ND/water interface revealed the formation of a strong hydrogen bond network responsible for fluorescence tuning and colloidal stability (Saberi-Movahed & Brenner, 2021). It was shown that negatively charged DND–COOH reveals dipole slowing and reorientational dynamics of hydroxyl groups at the aqueous interface independently of the concentrations of the dissolved ions. Thus, the charged surficial groups (ND-COOH) strongly reduce the reorientational dynamics of H_2O in various directions, influencing both the wettability and surface energies. This effect could be attributed to the strong C-H bonds formed at the surface of carboxylated nanodiamond. Next, Saberi-Movahed et al. (Saberi-Movahed & Brenner, 2021) showed increasing interactions of ND-COOH with cations in order as following: K^+, Na^+, Ca_2^+, Mg_2^+. Moreover, they reduced the mobility of water around ND-COOH particles solvating in the chloride solvent. The reduction effect was attributed mainly to divalent cations thanks to their high charge concentrations. The hydration shell was formed around ND-COOH particles supported by highly mobile divalent cations. Thus, the engineering of the ND surface chemistry and the surrounding environment plays a significant role in the electron transport, tuning interactions with the solvent and modifying the emission that is crucial for sensing and imaging applications.

4. Conclusions

In summary, the fluorescence behavior of NV-rich, carboxylated nanodiamonds in various suspensions/cocktails (aqueous dispersion system, comestible liquids media) was systemically investigated. NDs are recognized as biocompatible and safe materials with chemically flexible surfaces for a large variety of food products or their packaging. The fluorescence of NV-NDs would enable a targeted detection of food quality or monitoring of

preservation. The fluorescence of NDs depends strongly on the interactions with surrounding media, their pH and chemical activity. Thus, we have analyzed a wide pH range of comestible liquids to investigate their influence on the NDs' fluorescence and stability (surface free energy, zeta potential) towards future food-oriented applications. Durable nanodiamond particles could be also used in smart food packaging, enabling fluorescent monitoring of the quality of the stored food and preserving the shelf-life of food products delivering superhydrophobicity. The study of the influence of NDs on food products is additionally important due to the risk of release of the nanodiamonds from the packaging to the product. Optical addressing of the color centers and observation of their fluorescence may be used to verify the presence of NDs in the comestible products in a safe and non-contact way. However, the properties of the dispersion medium (e.g. its pH) may affect the performance of the particles suspended in it. Therefore, it is important to evaluate whether a composition of a certain comestible product does not hinder the fluorescence of the nanodiamonds, impeding the unambiguous identification of the characteristic peaks of the spectra (i.e. zero-phonon lines of NV centers). All the above-mentioned properties of fluorescent nanodiamonds, also taking into account their biocompatibility and durability, make them a good candidate for applications as biomarkers in food safety issues and life science.

The dried solutions of NV-ND suspensions revealed an increased effect of agglutination in higher pH delivered by green tea or alkaline water. The ND agglutinates exhibited a kind of core-shell softened morphology probably induced by spirit vinegar and green tea residuals. The aggregation effect was attributed to the variations of electrostatic forces between the NDs in various comestibles induced not only by their pHs, but also by various nature-originated compounds present in them. For optimum performance, NDs must retain their colloidal stability in designated dispersion media. The optical technique commonly used to evaluate colloidal stability of particles suspended in liquids is electrophoretic light scattering, used in this study to evaluate the stability of the suspensions by measuring the zeta potential. Furthermore, we have observed significant pH dependence of the ND-NV fluorescence tuned mainly by deprotonation of -COOH surficial groups. Deprotonated ND-COOH surfaces exhibit a large negative charge creating a dense hydration shell around particles by surrounding water molecules, which significantly quench the nanodiamond fluorescence.

The nanodiamond cocktails combined with complex organic comestibles influence the fluorescence signals mainly due to the pH of the samples. The selected comestibles such as vinegar, black tea, green tea interfere with the NV centers causing fluorescence quenching or overlapping the nanodiamond emission. It is noteworthy that a significant boosting effect was observed for lemon juice, which is responsible for increased electrical conductivity and wettability, facilitating enhanced fluorescence. On the other hand, beetroot juice caused strong nanodiamond fluorescence extinction attributed to the betanin pigment and betalains derivatives present in the natural extract. Other nature-originated compounds such as the catechin, caffeine, and theaflavin present in green and black teas also decreased nanodiamond fluorescence as they are static quenchers. Overall, micro-molar concentrations of

metal ions such as Sn(II) and Zn(II) could induce quenching behavior when weakly bonded or adsorbed at the nanodiamond surface. This phenomenon could be also applied for further studies of heavy metal cations detection in food products.

Next, the impact of the presence of nanodiamonds on the parameters of wettability and surface tension of the liquids, related to the pH of the tested systems, was also presented. Such an approach allowed us to gain an understanding of solvent/nanodiamond interactions driving fluorescence variations. The admixture of nanodiamond suspensions into these samples reduces surface tension, mostly due to the Brownian motion of nanoparticles within the comestible liquid. Generally, comestibles with an acid nature exhibit better wettability of a dispersive material such as PTFE than those of an alkaline nature. The presence of nanodiamond particles lowers this property, which can be caused by the adsorption of the nanoparticles on the PTFE surface, thus changing the solid-liquid interface. Furthermore, measurements of wettability and contact angle of ND-based comestible suspensions could be utilized to monitor food composition or its degradation improving food processing and storage technologies.

Finally, the achieved results manifested that fluorescent, NV-rich nanodiamond particles are stable in liquid comestibles that could be utilized for optical food quality and safety monitoring. Next, the studies focused on spin properties or charge-state dynamics of nitrogen vacancies in nanodiamonds would also enable magnetic sensing or imaging applications. The flexible biochemical nature and biocompatibility of nanodiamond surfaces enable further research on the intelligent delivery-mediated nutraceuticals, smart food protection by nanosensing and tailored preserving using their customized and fluorescent functionalities.

Acknowledgments

This research work has been supported by the Foundation for Polish Science under grant no. POIR.04.04.00-00-1644/18. The authors would like to thank Mr. Piotr Krystosiak from A.P. Instruments Sp. z o.o. Sp. k. for measuring the zeta potential of the diamond suspensions based on the comestible liquids.

Notes

The authors declare no competing financial interests.

References

Arcot, Y., Liu, S., Ulugun, B., DeFlorio, W., Bae, M., Salazar, K. S., Taylor, T. M., Castillo, A., Cisneros-Zevallos, L., & Scholar, E. M. A. (2021). Fabrication of Robust Superhydrophobic Coatings onto

High-Density Polyethylene Food Contact Surfaces for Enhanced Microbiological Food Safety. *ACS Food Science & Technology*, *1*(7), 1180–1189. https://doi.org/10.1021/acsfoodscitech.1c00082

Babadi, F. E., Hosseini, S., Shavandi, A., Moghaddas, H., Shotipruk, A., & Kheawhom, S. (2019). Electrochemical investigation of amino acids Parkia seeds using the composite electrode based on copper/carbon nanotube/nanodiamond. *Journal of Environmental Chemical Engineering*, *7*(2), 102979. https://doi.org/10.1016/j.jece.2019.102979

Bhaumik, A., Sachan, R., & Narayan, J. (2019). Tunable charge states of nitrogen-vacancy centers in diamond for ultrafast quantum devices. *Carbon*, *142*, 662–672. https://doi.org/10.1016/j.carbon.2018.10.084

Białobrzeska, W., Głowacki, M. J., Janik, M., Ficek, M., Pyrchla, K., Sawczak, M., Bogdanowicz, R., Malinowska, N., Żołędowska, S., & Nidzworski, D. (2021). Quantitative fluorescent determination of DNA – Ochratoxin a interactions supported by nitrogen-vacancy rich nanodiamonds. *Journal of Molecular Liquids*, *342*, 117338. https://doi.org/10.1016/j.molliq.2021.117338

Bradac, C., Rastogi, I. D., Cordina, N. M., Garcia-Bennett, A., & Brown, L. J. (2018). Influence of surface composition on the colloidal stability of ultra-small detonation nanodiamonds in biological media. *Diamond and Related Materials*, *83*, 38–45. https://doi.org/10.1016/j.diamond.2018.01.022

Carvalho, A., Freitas, M., Nouws, H. P. A., & Delerue-Matos, C. (2021). A Voltammetric Nanodiamond-Coated Screen-Printed Immunosensor for The Determination of a Peanut Allergen in Commercial Food Products. *Chemistry Proceedings*, *5*(1), 10. https://doi.org/10.3390/CSAC2021-10458

Choi, J., Yong, K., Choi, J., & Cowie, A. (2019). Emerging Point-of-care Technologies for Food Safety Analysis. *Sensors*, *19*(4), 817. https://doi.org/10.3390/s19040817

Cong, S., Wang, N., Wang, K., Wu, Y., Li, D., Song, Y., Prakash, S., & Tan, M. (2019). Fluorescent nanoparticles in the popular pizza: Properties, biodistribution and cytotoxicity. *Food & Function*, *10*(5), 2408–2416. https://doi.org/10.1039/C8FO01944D

Crane, M. J., Petrone, A., Beck, R. A., Lim, M. B., Zhou, X., Li, X., Stroud, R. M., & Pauzauskie, P. J. (2019). High-pressure, high-temperature molecular doping of nanodiamond. *Science Advances*, *5*(5), eaau6073. https://doi.org/10.1126/sciadv.aau6073

Cui, B., Liu, H., Yu, H., Pang, X., Yan, H., & Bai, L. (2019). Monolithic Material Prepared with Nanodiamond as Monomer for the Enrichment of β-Sitosterol in Edible Oil. *Food Analytical Methods*, *12*(3), 697–704. https://doi.org/10.1007/s12161-018-1405-9

Das, A., De, D., Ghosh, A., & Goswami, M. M. (2020). An innovative cell imaging by beet root extracted pigment. *Spectrochimica Acta Part A: Molecular and Biomolecular Spectroscopy*, *230*, 118037. https://doi.org/10.1016/j.saa.2020.118037

Du, C., Ma, C., Gu, J., Li, L., & Chen, G. (2020). Fluorescence Sensing of Caffeine in Tea Beverages with 3,5-diaminobenzoic Acid. *Sensors*, *20*(3), 819. https://doi.org/10.3390/s20030819

Du, C., Ma, C., Gu, J., Li, L., Zhu, C., Chen, L., Wang, T., & Chen, G. (2020). Rapid Determination of Catechin Content in Black Tea by Fluorescence Spectroscopy. *Journal of Spectroscopy*, *2020*, 1–8. https://doi.org/10.1155/2020/2479612

Dutta Choudhury, S., Chethodil, J. M., Gharat, P. M., P. K., P., & Pal, H. (2017). pH-Elicited Luminescence Functionalities of Carbon Dots: Mechanistic Insights. *The Journal of Physical Chemistry Letters*, *8*(7), 1389–1395. https://doi.org/10.1021/acs.jpclett.7b00153

Ferdous, S., Ioannidis, M. A., & Henneke, D. E. (2012). Effects of temperature, pH, and ionic strength on the adsorption of nanoparticles at liquid–liquid interfaces. *Journal of Nanoparticle Research*, *14*(5), 850. https://doi.org/10.1007/s11051-012-0850-4

Fujisaku, T., Tanabe, R., Onoda, S., Kubota, R., Segawa, T. F., So, F. T.-K., Ohshima, T., Hamachi, I., Shirakawa, M., & Igarashi, R. (2019). PH Nanosensor Using Electronic Spins in Diamond. *ACS Nano*, *13*(10), 11726–11732. https://doi.org/10.1021/acsnano.9b05342

Fujiwara, M., Tsukahara, R., Sera, Y., Yukawa, H., Baba, Y., Shikata, S., & Hashimoto, H. (2019). Monitoring spin coherence of single nitrogen-vacancy centers in nanodiamonds during pH changes in aqueous buffer solutions. *RSC Advances*, *9*(22), 12606–12614. https://doi.org/10.1039/C9RA02282A

Gargouri, B., Ammar, S., Verardo, V., Besbes, S., Segura-Carretero, A., & Bouaziz, M. (2017). RP-HPLC–DAD-ESI-TOF–MS based strategy for new insights into the qualitative and quantitative phenolic profile in Tunisian industrial Citrus Limon by-product and their antioxidant activity. *European Food Research and Technology*, *243*(11), 2011–2024. https://doi.org/10.1007/s00217-017-2904-4

Gliszczyńska-Świgło, A., Szymusiak, H., & Malinowska, P. (2006). Betanin, the main pigment of red beet: Molecular origin of its exceptionally high free radical-scavenging activity. *Food Additives and Contaminants*, *23*(11), 1079–1087. https://doi.org/10.1080/02652030600986032

Grichko, V., Grishko, V., & Shenderova, O. (2006). Nanodiamond bullets and their biological targets. *NanoBiotechnology*, *2*(1–2), 37–42. https://doi.org/10.1007/s12030-006-0005-8

Jiang, L., Santiago, I., & Foord, J. (2018). Nanocarbon and nanodiamond for high performance phenolics sensing. *Communications Chemistry*, *1*(1), 43. https://doi.org/10.1038/s42004-018-0045-8

Kumar, A., & Dixit, C. K. (2017). Methods for characterization of nanoparticles. In *Advances in Nanomedicine for the Delivery of Therapeutic Nucleic Acids* (pp. 43–58). Elsevier. https://doi.org/10.1016/B978-0-08-100557-6.00003-1

Kumar, V., Kaur, I., Arora, S., Mehla, R., Vellingiri, K., & Kim, K.-H. (2020). Graphene nanoplatelet/graphitized nanodiamond-based nanocomposite for mediator-free electrochemical sensing of urea. *Food Chemistry*, *303*, 125375. https://doi.org/10.1016/j.foodchem.2019.125375

Lei, Y., Zheng, M.-L., Zhao, Z.-S., & Duan, X.-M. (2016). Carboxylated Nanodiamond: Aggregation Properties in Aqueous Dispersion System and Application in Living Cell Fluorescence Imaging. *Journal of Nanoscience and Nanotechnology*, *16*(3), 2319–2324. https://doi.org/10.1166/jnn.2016.10932

Li, B., Zhang, Z., Qi, J., Zhou, N., Qin, S., Choo, J., & Chen, L. (2017). Quantum Dot-Based Molecularly Imprinted Polymers on Three-Dimensional Origami Paper Microfluidic Chip for Fluorescence Detection of Phycocyanin. *ACS Sensors*, *2*(2), 243–250. https://doi.org/10.1021/acssensors.6b00664

Li, Y., Feng, Z., Li, Y., Jin, W., Peng, Q., Zhang, P., He, J., & Li, K. (2020). Metal ions-triggered photo-induced fluorescence change in rhodamine B-based photo-responsive complexes. *Spectrochimica Acta Part A: Molecular and Biomolecular Spectroscopy*, *230*, 118069. https://doi.org/10.1016/j.saa.2020.118069

Lim, D. G., Jung, J. H., Ko, H. W., Kang, E., & Jeong, S. H. (2016). Paclitaxel–Nanodiamond Nanocomplexes Enhance Aqueous Dispersibility and Drug Retention in Cells. *ACS Applied Materials & Interfaces*, *8*(36), 23558–23567. https://doi.org/10.1021/acsami.6b08079

Lim, D. G., Kang, E., & Jeong, S. H. (2020). PH-dependent nanodiamonds enhance the mechanical properties of 3D-printed hyaluronic acid nanocomposite hydrogels. *Journal of Nanobiotechnology*, *18*(1), 88. https://doi.org/10.1186/s12951-020-00647-w

Lim, D. G., Rajasekaran, N., Lee, D., Kim, N. A., Jung, H. S., Hong, S., Shin, Y. K., Kang, E., & Jeong, S. H. (2017). Polyamidoamine-Decorated Nanodiamonds as a Hybrid Gene Delivery Vector and

siRNA Structural Characterization at the Charged Interfaces. *ACS Applied Materials & Interfaces*, *9*(37), 31543–31556. https://doi.org/10.1021/acsami.7b09624

Lim, S., Horiuchi, H., Nikolov, A. D., & Wasan, D. (2015). Nanofluids Alter the Surface Wettability of Solids. *Langmuir*, *31*(21), 5827–5835. https://doi.org/10.1021/acs.langmuir.5b00799

Ma, Z.-C., Gao, N., Cheng, S.-H., Liu, J.-S., Yang, M.-C., Wang, P., Feng, Z.-Y., Wang, Q.-L., & Li, H.-D. (2020). Wettability and Surface Energy of Hydrogen- and Oxygen-Terminated Diamond Films. *Chinese Physics Letters*, *37*(4), 046801. https://doi.org/10.1088/0256-307X/37/4/046801

Medeiros, R. A., Rocha-Filho, R. C., & Fatibello-Filho, O. (2010). Simultaneous voltammetric determination of phenolic antioxidants in food using a boron-doped diamond electrode. *Food Chemistry*, *123*(3), 886–891. https://doi.org/10.1016/j.foodchem.2010.05.010

Miao, M., Jiang, B., Jiang, H., Zhang, T., & Li, X. (2015). Interaction mechanism between green tea extract and human α-amylase for reducing starch digestion. *Food Chemistry*, *186*, 20–25. https://doi.org/10.1016/j.foodchem.2015.02.049

Mikamoto, K., Nishitani, T., Tsubaki, Y., Shirakura, A., & Suzuki, T. (2020). Improvement of durability and sliding properties of food packaging equipment by combined treatment of diamond-like carbon coating and fine particle bombarding. *Journal of Applied Packaging Research*, *12*(1), 54–62.

Mitura, K., Wyre˛bski, K., & Zarzycki, P. K. (2017). Bioactive food packaging with nanodiamond particles manufactured by detonation and plasma-chemical methods. In *Food Packaging* (pp. 295–328). Elsevier. https://doi.org/10.1016/B978-0-12-804302-8.00009-1

Ostrovskaya, L. Y. (2002). Studies of diamond and diamond-like film surfaces using XAES, AFM and wetting. *Vacuum*, *68*(3), 219–238. https://doi.org/10.1016/S0042-207X(02)00460-8

Ozdemir, S., Kilinc, E., Celik, K. S., Okumus, V., & Soylak, M. (2017). Simultaneous preconcentrations of Co2+, Cr6+, Hg2+ and Pb2+ ions by Bacillus altitudinis immobilized nanodiamond prior to

their determinations in food samples by ICP-OES. *Food Chemistry*, *215*, 447–453. https://doi.org/10.1016/j.foodchem.2016.07.055

Panwar, N., Soehartono, A. M., Chan, K. K., Zeng, S., Xu, G., Qu, J., Coquet, P., Yong, K.-T., & Chen, X. (2019). Nanocarbons for Biology and Medicine: Sensing, Imaging, and Drug Delivery. *Chemical Reviews*, *119*(16), 9559–9656. https://doi.org/10.1021/acs.chemrev.9b00099

Radiom, M., Yang, C., & Chan, W. K. (2009). *Characterization of surface tension and contact angle of nanofluids* (C. Quan, K. Qian, A. K. Asundi, & F. S. Chau, Eds.; p. 75221D). https://doi.org/10.1117/12.851278

Reineck, P., Lau, D. W. M., Wilson, E. R., Nunn, N., Shenderova, O. A., & Gibson, B. C. (2018). Visible to near-IR fluorescence from single-digit detonation nanodiamonds: Excitation wavelength and pH dependence. *Scientific Reports*, *8*(1), 2478. https://doi.org/10.1038/s41598-018-20905-0

Reinke, S. K., Hauf, K., Vieira, J., Heinrich, S., & Palzer, S. (2015). Changes in contact angle providing evidence for surface alteration in multi-component solid foods. *Journal of Physics D: Applied Physics*, *48*(46), 464001. https://doi.org/10.1088/0022-3727/48/46/464001

Rondin, L., Dantelle, G., Slablab, A., Grosshans, F., Treussart, F., Bergonzo, P., Perruchas, S., Gacoin, T., Chaigneau, M., Chang, H.-C., Jacques, V., & Roch, J.-F. (2010). Surface-induced charge state conversion of nitrogen-vacancy defects in nanodiamonds. *Physical Review B*, *82*(11), 115449. https://doi.org/10.1103/PhysRevB.82.115449

Saberi-Movahed, F., & Brenner, D. W. (2021). Impacts of surface chemistry and adsorbed ions on dynamics of water around detonation nanodiamond in aqueous salt solutions. *ArXiv:2102.13312 [Cond-Mat, Physics:Physics]*. http://arxiv.org/abs/2102.13312

Sacksteder, L., Ballew, R. M., Brown, E. A., Demas, J. N., Nesselrodt, D., & DeGraff, B. A. (1990). Photophysics in a disco: Luminescence quenching of quinine. *Journal of Chemical Education*, *67*(12), 1065. https://doi.org/10.1021/ed067p1065

638 Sefiane, K., Skilling, J., & MacGillivray, J. (2008). Contact line motion and dynamic wetting of nanofluid
639 solutions. *Advances in Colloid and Interface Science*, *138*(2), 101–120.
640 https://doi.org/10.1016/j.cis.2007.12.003
641 Shabnam, L., Faisal, S. N., Roy, A. K., Haque, E., Minett, A. I., & Gomes, V. G. (2017). Doped
642 graphene/Cu nanocomposite: A high sensitivity non-enzymatic glucose sensor for food. *Food*
643 *Chemistry*, *221*, 751–759. https://doi.org/10.1016/j.foodchem.2016.11.107
644 Tsapyuk, G. G., Diyuk, V. E., Mariychuk, R., Panova, A. N., Loginova, O. B., Grishchenko, L. M.,
645 Dyachenko, A. G., Linnik, R. P., Zaderko, A. N., & Lisnyak, V. V. (2020). Effect of ultrasonic
646 treatment on the thermal oxidation of detonation nanodiamonds. *Applied Nanoscience*, *10*(12),
647 4991–5001. https://doi.org/10.1007/s13204-020-01277-2
648 Ulusoy, H. İ., Gülle, S., Yilmaz, E., & Soylak, M. (2019). Trace determination of vitamin B12 in food
649 samples by using Fe_3O_4 magnetic particles including multi-walled carbon nanotubes and
650 nanodiamonds. *Analytical Methods*, *11*(40), 5108–5117. https://doi.org/10.1039/C9AY01504C
651 Vafaei, S., Borca-Tasciuc, T., Podowski, M. Z., Purkayastha, A., Ramanath, G., & Ajayan, P. M. (2006).
652 Effect of nanoparticles on sessile droplet contact angle. *Nanotechnology*, *17*(10), 2523–2527.
653 https://doi.org/10.1088/0957-4484/17/10/014
654 Wu, D., Mei, S., Duan, R., Geng, F., Wu, W., Li, X., Cheng, L., & Wang, C. (2020). How black tea
655 pigment theaflavin dyes chicken eggs: Binding affinity study of theaflavin with ovalbumin. *Food*
656 *Chemistry*, *303*, 125407. https://doi.org/10.1016/j.foodchem.2019.125407
657 Zelent, B., Vanderkooi, J. M., Coleman, R. G., Gryczynski, I., & Gryczynski, Z. (2006). Protonation of
3 Excited State Pyrene-1-Carboxylate by Phosphate and Organic Acids in Aqueous Solution
9 Studied by Fluorescence Spectroscopy. *Biophysical Journal*, *91*(10), 3864–3871.
0 https://doi.org/10.1529/biophysj.106.088740

Zhong, X., Crivoi, A., & Duan, F. (2015). Sessile nanofluid droplet drying. *Advances in Colloid and Interface Science*, *217*, 13–30. https://doi.org/10.1016/j.cis.2014.12.003

Zhuang, H., Song, B., Srikanth, V. V. S. S., Jiang, X., & Schönherr, H. (2010). Controlled Wettability of Diamond/β-SiC Composite Thin Films for Biosensoric Applications. *The Journal of Physical Chemistry C*, *114*(47), 20207–20212. https://doi.org/10.1021/jp109093h